

Carbonyl Derivatives of Chloride–Dimethyl Sulfoxide–Ruthenium(III) Complexes: Synthesis, Crystal Structure, and Reactivity of [(DMSO)₂H][*trans*-RuCl₄(DMSO)(CO)] and *mer,cis*-RuCl₃(DMSO)₂(CO)

E. Alessio,^{*,†} M. Bolle,[†] B. Milani,[†] G. Mestroni,[†] P. Faleschini,[†] S. Geremia,[‡] and M. Calligaris^{*,†}

Dipartimento di Scienze Chimiche, Università di Trieste, Via L. Giorgieri 1, 34127 Trieste, Italy, and Dipartimento di Scienze dei Materiali e della Terra, Università di Ancona, Via delle Brece Bianche, Ancona, Italy

Received December 22, 1994[®]

The synthesis, spectroscopic characterization and crystal structure of [(DMSO)₂H][*trans*-RuCl₄(DMSO)(CO)] (**3**) and *mer,cis*-RuCl₃(DMSO)₂(CO) (**4**) are reported (DMSO = O-bonded dimethyl sulfoxide). The two complexes are easily synthesized from [(DMSO)₂H][*trans*-RuCl₄(DMSO)₂] (**1**) and *mer,trans*-RuCl₃(DMSO)₂(DMSO) (**2**), respectively, upon reaction with carbon monoxide at room temperature and atmospheric pressure. They represent the first examples of Ru(III) chloride–DMSO–carbonyl complexes. Coordination of carbon monoxide induces the S to O linkage isomerization of the DMSO ligand trans to it. [(DMSO)₂H][*trans*-RuCl₄(DMSO)(CO)]: orthorhombic, space group *Pnma*, *Z* = 4, *a* = 10.564(1) Å, *b* = 14.620(3) Å, *c* = 12.312(1) Å. *mer,cis*-RuCl₃(DMSO)₂(CO): triclinic, space group *P1*, *Z* = 4, *a* = 6.991(9) Å, *b* = 13.98(1) Å, *c* = 14.86(2) Å, $\alpha = 82.76(8)^\circ$, $\beta = 85.83(8)^\circ$, $\gamma = 75.41(9)^\circ$. In both **3** and **4** the DMSO ligand trans to CO is weakly bonded and easily replaced by a nitrogen donor ligand such as NH₃ or pyridine.

Introduction

As a part of our detailed investigation of the chemistry of ruthenium–DMSO complexes,^{1–5} we have recently described the reactivity of [(DMSO)₂H][*trans*-RuCl₄(DMSO)₂] (**1**) and *mer,trans*-RuCl₃(DMSO)₂(DMSO) (**2**) (DMSO = S-bonded sulfoxide, DMSO = O-bonded sulfoxide) with σ -donor ligands.⁶ The structural and spectroscopic evidence collected to date and comparison with the corresponding Rh(III) derivatives^{7,8} led us to formulate the hypothesis that the ruthenium–sulfur bond of DMSO has a relevant metal-to-ligand π component not only in Ru(II) but also in Ru(III) compounds. In order to test this hypothesis and assess the effect of π -back-bonding competition on the Ru(III)–DMSO bond, we decided to investigate the reactivity of **1** and **2** with a π -acceptor ligand such as carbon monoxide. This led us to the isolation of two new stable Ru(III) carbonyl derivatives, [(DMSO)₂H][*trans*-RuCl₄(DMSO)(CO)] (**3**) and *mer,cis*-RuCl₃(DMSO)₂(CO) (**4**), whose synthesis, spectroscopic characterization, and crystal structure are reported here. It should be noted that coordination of carbon monoxide induces a linkage isomerization (S/O) of the remaining DMSO trans to it.

Even though an Os(III) compound isostructural to **3** has been recently described,⁹ to our knowledge these are the first examples of Ru(III) compounds bearing both DMSO and CO.

The new complexes represent also an important contribution to the rather limited chemistry of monomeric Ru(III)–carbonyl complexes described in the literature.¹⁰ In fact, beside the long known [RuCl₅(CO)]²⁻, [RuBr₅(CO)]²⁻, and [pyH][RuCl₄(CO)(py)], whose syntheses were reported in the 1960s,^{11–13} the only other example of Ru(III)–carbonyl complexes concerns the cationic Schiff base–carbonyl complexes described more recently by Taqui Khan and co-workers.¹⁴

Experimental Section

Material. Analytical grade solvents (Baker) were used without further purification for synthetic purposes. RuCl₃·3H₂O was obtained from Johnson Matthey. Deuterated solvents for NMR were purchased from Aldrich.

Physical Measurements. Electronic absorption spectra were recorded in stoppered quartz cells with a Perkin-Elmer Lambda 5 UV/vis spectrophotometer equipped with a thermostat. Unless otherwise stated, spectra were recorded immediately after dissolution of the complexes. Solid state infrared spectra were obtained as Nujol mulls on a Perkin-Elmer 983G spectrometer. ¹H NMR spectra were recorded at 400 MHz on a JEOL EX400 FT instrument. All spectra were run at room temperature with tetramethylsilane (TMS) as an internal reference for CD₂Cl₂ and CDCl₃ solutions and sodium 2,2-dimethyl-2-silapentane (DSS) for D₂O solutions. Elemental analyses were performed by Dr. E. Cebulec (Dipartimento Scienze Chimiche, Università di Trieste).

[†]Università di Trieste.

[‡]Università di Ancona.

[®] Abstract published in *Advance ACS Abstracts*, August 1, 1995.

- (1) Alessio, E.; Mestroni, G.; Nardin, G.; Attia, W. M.; Calligaris, M.; Sava, G.; Zorzet, S. *Inorg. Chem.* **1988**, *27*, 4099.
- (2) Alessio, E.; Milani, B.; Mestroni, G.; Calligaris, M.; Faleschini, P.; Attia, W. M. *Inorg. Chim. Acta* **1990**, *177*, 255.
- (3) Henn, M.; Alessio, E.; Mestroni, G.; Calligaris, M.; Attia, W. M. *Inorg. Chim. Acta* **1991**, *187*, 39.
- (4) Alessio, E.; Milani, B.; Calligaris, M.; Bresciani-Pahor, N. *Inorg. Chim. Acta* **1992**, *194*, 85.
- (5) Alessio, E.; Balducci, G.; Calligaris, M.; Costa, G.; Attia, W. M.; Mestroni, G. *Inorg. Chem.* **1991**, *30*, 609.
- (6) Alessio, E.; Balducci, G.; Lutman, A.; Mestroni, G.; Calligaris, M.; Attia, W. M. *Inorg. Chim. Acta* **1993**, *203*, 205.
- (7) Alessio, E.; Faleschini, P.; Sessanta o Santi, A.; Mestroni, G.; Calligaris, M. *Inorg. Chem.* **1993**, *32*, 5756.
- (8) Alessio, E.; Sessanta o Santi, A.; Faleschini, P.; Calligaris, M.; Mestroni, G. *J. Chem. Soc., Dalton Trans.* **1994**, 1849.

(9) Johnson, T. W.; Tetrick, S. M.; Fanwick, P. E.; Walton, R. A. *Inorg. Chem.* **1991**, *30*, 4146.

(10) Seddon, E. A.; Seddon, K. R. In *The Chemistry of Ruthenium*; Clark, R. J. H., Ed.; Elsevier: Amsterdam, The Netherlands, 1984.

(11) Halpern, J.; James, B. R.; Kemp, L. W. *J. Am. Chem. Soc.* **1966**, *88*, 5142.

(12) Colton, R.; Farthing, R. H. *Aust. J. Chem.* **1971**, *24*, 903.

(13) Stephenson, T. A.; Wilkinson, G. *J. Inorg. Nucl. Chem.* **1966**, *28*, 945.

(14) Taqui Khan, M. M.; Srinivas, D.; Kureshy, R. I.; Khan, N. H. *Inorg. Chem.* **1990**, *29*, 2320.

Synthesis of the Complexes. [(DMSO)₂H][*trans*-RuCl₄(DMSO)₂] (1), its sodium salt (1Na), and *mer,trans*-RuCl₃(DMSO)₂(DMSO) (2) were synthesized and recrystallized according to the procedure reported in ref 5.

The tetrabutylammonium derivative of 1, [NBu₄][*trans*-RuCl₄(DMSO)₂] (1NBu₄), was synthesized according to the following procedure: a 1 g amount of 1 (1.8 mmol) was dissolved in 5 mL of water and a 2-fold excess of tetrabutylammonium chloride dissolved in the minimum amount of water was added dropwise. A precipitate of the product rapidly formed and was filtered off, washed with water, cold acetone and diethyl ether, and vacuum dried. Yield: 80%. Anal. Calcd for C₂₀H₄₈NCl₄O₂RuS₂ (*M_r* = 641.61): C, 37.44; H, 7.54; N, 2.18. Found: C, 37.6; H, 7.64; N, 2.17.

[(DMSO)₂H][*trans*-RuCl₄(DMSO)(CO)] (3). A 0.3 g amount of 1 (0.54 mmol) was partially dissolved in 0.5 mL of DMSO and 5 mL of acetone in a flask closed with a stopcock. The flask was first connected to a vacuum line and then to a reservoir of CO. The mixture was reacted for 7 h at room temperature; during this time the starting material dissolved completely and the orange solution gradually turned deep-red. Microcrystals of the same color formed in a few hours from the solution stored at 4 °C, after concentration to approximately 3 mL and addition of some diethyl ether. They were filtered off, rapidly washed with cold acetone and diethyl ether, and vacuum dried. A second fraction of the product precipitated from the concentrated mother liquor upon further addition of diethyl ether. Total yield: 0.16 g (60%). Anal. Calcd for C₇H₁₉Cl₄O₄RuS₃ (*M_r* = 506.28): C, 16.6; H, 3.78; S, 18.99. Found: C, 16.4; H, 3.68; S, 19.1. UV/visible spectra (*λ*_{max}, nm (ε, M⁻¹cm⁻¹)): in DMSO solution, 557 (388), 468 (4857), 395 (sh) (1096), 317 (sh) (1500). Selected IR absorption bands: Nujol, ν_{CO} 2030 cm⁻¹ (vs), ν_{SO} 957 cm⁻¹ (s) (DMSO), ν_{O-H-O} 735 cm⁻¹ (s, vb) ((DMSO)₂H⁺), ν_{Ru-C} 503 cm⁻¹ (w), ν_{Ru-O} 461 cm⁻¹ (m), ν_{Ru-Cl} 320 cm⁻¹ (s); DMSO-*d*₆ derivative (isotope ratio), ν_{SO} 962 cm⁻¹ (s) (DMSO), ν_{Ru-O} 429 cm⁻¹ (m) (1.07).

Na[*trans*-RuCl₄(DMSO)(CO)]·2DMSO (3Na). A 0.3 g amount of Na[*trans*-RuCl₄(DMSO)₂] (0.7 mmol) was partially dissolved in 0.5 mL of DMSO and 10 mL of acetone and reacted with CO as described above. After 5 h the deep red solution was filtered over fine paper and some diethyl ether added. Deep-red crystals of the product formed in a few hours and were filtered, rapidly washed with cold acetone and diethyl ether and vacuum dried at room temperature. Yield: 0.16 g (42%). Anal. Calcd for C₇H₁₈Cl₄NaO₄RuS₃ (*M_r* = 528.26): C, 15.91; H, 3.43; S, 18.20. Found: C, 15.5; H, 3.42; S, 18.0. Selected IR absorption bands: Nujol, ν_{CO} 2047 cm⁻¹ (vs), ν_{SO} 1032 cm⁻¹ (vs) (DMSO), ν_{SO} 928 cm⁻¹ (s) (DMSO), δ_{RuCO} 549 cm⁻¹ (m), ν_{Ru-C} 503 cm⁻¹ (w), ν_{Ru-O} 476 cm⁻¹ (m), ν_{Ru-Cl} 326 cm⁻¹ (vs); DMSO-*d*₆ derivative (isotope ratio), ν_{SO} 943 cm⁻¹ (s) (DMSO), δ_{RuCO} 550 cm⁻¹ (m), ν_{Ru-C} 503 cm⁻¹ (w), ν_{Ru-O} 450 cm⁻¹ (m) (1.05).

[NBu₄][*trans*-RuCl₄(DMSO)(CO)] (3NBu₄). A 0.25 g amount of [NBu₄][*trans*-RuCl₄(DMSO)₂] (0.39 mmol) was dissolved in 10 mL of CHCl₃ and reacted with CO as described above. After 5 h, the deep-red solution was concentrated to an oil, which was redissolved in 3 mL of acetone and stored at 4 °C. The product precipitated as deep-red crystals after addition of some diethyl ether. It was filtered, washed with diethyl ether, and vacuum dried. Yield: 0.18 g (80%). Anal. Calcd for C₁₉H₄₂NCl₄O₂RuS (*M_r* = 591.49): C, 38.58; H, 7.15; N, 2.36; S, 5.42. Found: C, 38.4; H, 7.13; N, 2.32; S, 5.4. UV/visible spectra (*λ*_{max}, nm (ε, M⁻¹cm⁻¹)): in CHCl₃ solution, 554 (444), 460 (6095), 323 (1978), 262 (7679). Selected IR absorption bands: Nujol, ν_{CO} 2024 cm⁻¹ (vs), ν_{SO} 954 cm⁻¹ (s) (DMSO), ν_{Ru-O} 465 cm⁻¹ (m), ν_{Ru-Cl} 324 cm⁻¹ (vs); (CHCl₃ solution), ν_{CO} 2038 cm⁻¹ (vs). Selected NMR resonances (δ): CDCl₃, -0.2 ppm (vb) (DMSO).

mer,cis-RuCl₃(DMSO)₂(CO) (4). A 0.51 g amount of 2 (1.15 mmol) was dissolved in 9 mL of CH₂Cl₂ and reacted with CO as described above. The initially orange solution turned gradually deep-red. After 6 h of reaction at room temperature, the solution was concentrated to approx 5 mL and then cooled to 4 °C after addition of some diethyl ether. Deep-red crystals of the product formed in a few hours and were filtered off, washed with cold CH₂Cl₂ and diethyl ether, and vacuum dried. Yield: 0.32 g (70%). Anal. Calcd for C₅H₁₂Cl₃O₃RuS₂ (*M_r* = 391.69): C, 15.33; H, 3.08; S, 16.36. Found: C, 15.2; H, 2.98; S, 16.3. UV/visible spectra (*λ*_{max}, nm (ε, M⁻¹cm⁻¹)): in chloroform solution, 504 (1065), 418 (3417), 305 (sh) (1497).

Selected IR absorption bands: Nujol, ν_{CO} 2044 cm⁻¹ (vs), ν_{SO} 932 and 885 cm⁻¹ (s) or 914 cm⁻¹ (vs, br) (DMSO), δ_{RuCO} 550 cm⁻¹ (m), ν_{Ru-O} 510 and 485 cm⁻¹ (m), ν_{Ru-Cl} 339 cm⁻¹ (vs); (CHCl₃): ν_{CO} 2053 cm⁻¹ (s); DMSO-*d*₆ derivative (isotope ratio), Nujol, ν_{SO} 941 and 907 cm⁻¹ (s) (DMSO), δ_{RuCO} 550 cm⁻¹ (m), ν_{Ru-C} 500 cm⁻¹ (w), ν_{Ru-O} 471 and 447 cm⁻¹ (m) (1.08). NMR resonances (δ): CDCl₃, 7.20 and -0.33 ppm (vb) (DMSO); CD₂Cl₂, 6.95 and -0.30 ppm (vb) (DMSO).

[NBu₄][*trans*-RuCl₄(NH₃)(CO)] (5NBu₄). A 0.25 g amount of 3NBu₄ (0.42 mmol) was dissolved in 10 mL of CH₂Cl₂ in a flask closed with a stopcock. The flask was first connected to a vacuum line and then swiftly to a reservoir of NH₃. The initially deep-red solution immediately lightened upon reaction with NH₃, whose excess was removed after 10 min. Orange-red microcrystals of the product formed from the solution stored at 4 °C, after concentration to half-volume and addition of some diethyl ether. They were filtered off, rapidly washed with cold CH₂Cl₂ and diethyl ether and vacuum dried. Yield: 0.11 g (50%). Anal. Calcd for C₁₇H₃₉N₂Cl₄ORu (*M_r* = 530.39): C, 38.49; H, 7.41; N, 5.28. Found: C, 37.9; H, 7.33; N, 5.14. UV/visible spectra (*λ*_{max}, nm (ε, M⁻¹cm⁻¹)): in chloroform solution, 534 (475), 443 (6313), 317 (2081), 260 (8897). Selected IR absorption bands: Nujol, ν_{NH} 3372 and 3260 (w), ν_{CO} 2025 cm⁻¹ (vs), δ_{RuCO} 538 cm⁻¹ (m), ν_{Ru-N} 483 (w), ν_{Ru-Cl} 320 cm⁻¹ (vs); (CHCl₃): ν_{CO} 2045 cm⁻¹ (vs).

mer-RuCl₃(NH₃)(CO)(DMSO) (6). A 0.32 g amount of complex 4 (0.82 mmol) was dissolved in 25 mL of CHCl₃ and reacted with NH₃ as described above. Also in this case the deep-red color of the solution immediately lightened upon reaction with ammonia and a small amount of a fluffy brown precipitate formed (to prevent its further increase, excess NH₃ was immediately removed). After filtration over fine paper, the mother liquor was concentrated to half-volume and some diethyl ether was added. Brick-red microcrystals of the product formed in a few hours and were filtered off, rapidly washed with cold CH₂Cl₂ and diethyl ether, and vacuum dried. Yield 0.15 g (55%). Anal. Calcd for C₃H₉NCl₃O₂RuS (*M_r* = 330.60): C, 10.89; H, 2.74; N, 4.23. Found: C, 10.8; H, 2.80; N, 4.30. UV/visible spectra (*λ*_{max}, nm (ε, M⁻¹cm⁻¹)): in chloroform solution, 493 (811), 410 (2146), 297 (sh) (1295). Selected IR absorption bands: Nujol, ν_{NH} 3324, 3249 and 3173 (w), ν_{CO} 2054 cm⁻¹ (vs), ν_{SO} 883 cm⁻¹ (s), δ_{RuCO} 534 cm⁻¹ (m), ν_{Ru-O} 513 cm⁻¹ (m), ν_{Ru-Cl} 331 cm⁻¹ (vs); (CHCl₃): ν_{CO} 2060 cm⁻¹ (vs); DMSO-*d*₆ derivative (isotope ratio), Nujol, ν_{SO} 884 cm⁻¹ (s) (DMSO), δ_{RuCO} 534 cm⁻¹ (m), ν_{Ru-O} 491 cm⁻¹ (m) (1.04).

Crystallographic Study. Crystals of 3 and 4 were obtained according to the procedures reported above, upon slowly increasing the amount of diethyl ether. Diffraction data were collected on an Enraf-Nonius CAD-4 fully automated four-circle diffractometer at ambient temperature. Unit cell parameters of both compounds were obtained from a least-squares fit of the setting angles of 25 machine-centered reflections. Graphite-monochromatized Mo K α radiation (λ = 0.710 69 Å) was used for data collection and cell dimension measurements. A summary of the crystal data and data collection and refinement is given in Table 1. Intensities were corrected for Lorentz–polarization factors, and an empirical absorption correction was also applied, by using the ψ -scan data of three close-to-axial reflections. Both structures were solved by the heavy-atom method through Patterson and Fourier syntheses. All hydrogen atoms were included at calculated positions. They were held fixed during refinement with isotropic *B* factors = 1.3*B*_{eq} of the carbon atoms to which they are bonded. The final full matrix least-squares refinement, with anisotropic temperature factors for all non-hydrogen atoms, converged to *R* = 0.030 for 3 and 0.038 for 4, respectively. Neutral atomic scattering factors and anomalous dispersion terms were taken from the literature.¹⁵ All calculations were performed by using the MolEN programs on a MicroVAX 2000 computer.¹⁶ The final coordinates of non-hydrogen atoms are listed in Tables 2 and 3 for 3 and 4, respectively. Bond lengths and angles are given in Tables 4 (3) and 5 (4). The labeling schemes for 3 and 4 are shown in Figures 2 and 3, respectively.

(15) *International Tables for Crystallography*; Kluwer Academic Publisher: Dordrecht, The Netherlands, 1992; Vol. C, Table 9.5.

(16) Fair, C. K. (1992). *MolEN. An Interactive Intelligent System for Crystal Structure Analysis*; Enraf-Nonius: Delft, The Netherlands, 1992.

Table 1. Crystallographic Data for **3** and **4**

	3	4
formula	C ₇ H ₁₉ Cl ₄ O ₄ RuS ₃	C ₅ H ₁₂ Cl ₃ O ₃ RuS ₂
<i>M_r</i>	506.3	391.7
cryst syst	orthorhombic	triclinic
space group	<i>Pnma</i>	<i>P1</i>
<i>a</i> , Å	10.564(1)	6.991(9)
<i>b</i> , Å	14.620(3)	13.98(1)
<i>c</i> , Å	12.312(1)	14.86(2)
α, deg	90	82.76(2)
β, deg	90	85.83(8)
γ, deg	90	75.41(9)
<i>V</i> , Å ³	1901.6(4)	1392
<i>Z</i>	4	4
<i>D</i> _{calc} , g cm ⁻³	1.77	1.87
μ(Mo Kα), cm ⁻¹	17.0	19.6
transm coeff	0.756–0.999	0.602–0.999
scan type	ω–2θ	ω–2θ
θ range, deg	3–30	3–27
no. of intens monitored ^a	3	3
no. of unique data no. with <i>I</i> > 3σ(<i>I</i>)	2802	5188
data/param ratio	19.7	20.4
<i>R</i> ^b	0.031	0.038
<i>R</i> _w ^c	0.030	0.038
GOF ^d	1.04	1.30

^a Measured after each 5000 s. ^b $R = \sum ||F_o| - |F_c|| / \sum |F_o|$. ^c $R_w = \sum [w(|F_o| - |F_c|)^2 / \sum w|F_o|^2]^{1/2}$. ^d $GOF = \{ \sum w(|F_o| - |F_c|)^2 / (m - n) \}^{1/2}$; *m* = no. of observations; *n* = no. of variables.

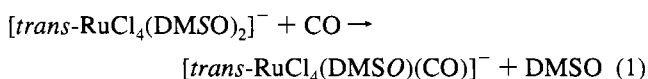
Table 2. Positional Parameters and *B* Values with Estimated Standard Deviations for **3**

atom	<i>x</i>	<i>y</i>	<i>z</i>	<i>B</i> _{<i>i</i>} , Å ²
Ru	0.16888(3)	0.250	0.50353(3)	2.826(4)
Cl1	0.1431(1)	0.250	0.69210(9)	5.02(2)
Cl2	0.1863(1)	0.250	0.31345(9)	5.16(3)
Cl3	0.1632(1)	0.09070(5)	0.50537(8)	6.10(2)
S1	-0.13628(9)	0.250	0.55015(9)	3.06(2) ^b
S2	0.0482(1)	0.02902(8)	0.17459(7)	5.02(2) ^c
O1	-0.0287(3)	0.250	0.4689(3)	4.80(8) ^b
O2	0.4463(3)	0.250	0.5243(5)	8.9(1)
O3	-0.0303(4)	-0.0249(3)	0.0916(2)	7.61(8) ^c
C1	-0.2356(4)	0.3402(2)	0.5053(4)	6.12(9)
C2	0.3400(4)	0.250	0.5174(4)	4.8(1)
C3	-0.0675(4)	0.0761(3)	0.2629(4)	6.7(1)
C4	0.1077(4)	-0.0573(3)	0.2570(4)	6.6(1)
S1B	-0.132(1)	0.250	0.4595(8)	4.3(2) ^d
S2B	-0.0338(5)	-0.0096(4)	0.1740(5)	4.02(9) ^e
O1B	-0.038(3)	0.250	0.539(2)	5.4(6) ^d
O3B	0.045(2)	0.054(1)	0.091(2)	6.5(4) ^e

^a Anisotropically refined atoms are given in the form of the isotropic equivalent displacement parameter defined as: $(4/3) [a^2\beta(1,1) + b^2\beta(2,2) + c^2\beta(3,3) + ab(\cos \gamma)\beta(1,2) + ac(\cos \beta)\beta(1,3) + bc(\cos \alpha)\beta(2,3)]$. ^b Occupancy factor = 0.88. ^c Occupancy factor = 0.86. ^d Isotropically refined with occupancy factor = 0.12. ^e Isotropically refined with occupancy factor = 0.14.

Results

[(DMSO)₂H][*trans*-RuCl₄(DMSO)₂] (**1**) reacts quite easily with carbon monoxide at room temperature and atmospheric pressure by replacing one of the two *trans* S-bonded DMSO ligands to give [(DMSO)₂H][*trans*-RuCl₄(DMSO)(CO)] (**3**) (eq 1). The reaction involves a rather large red-shift (approximately



50 nm) of the electronic absorption spectrum of the complex, whose shape remains however almost unchanged (Figure 1a). The same reaction occurs with the sodium or tetrabutylammonium salts of **1**, yielding **3Na** and **3NBu₄**, respectively.

Table 3. Positional Parameters and *B* Values with Estimated Standard Deviations for **4** (Two Independent Molecules (A and B) Present in the Unit Cell)

atom	<i>x</i>	<i>y</i>	<i>z</i>	<i>B</i> _{<i>i</i>} , Å ²
Molecule A				
Ru	0.07154(5)	0.22575(3)	0.90175(2)	3.598(7)
Cl1	0.3358(2)	0.1746(1)	0.79914(9)	5.23(3)
Cl2	-0.1687(2)	0.2822(1)	1.0132(1)	5.23(3)
Cl3	-0.1244(2)	0.3120(1)	0.78526(9)	5.96(3)
S1	0.4307(2)	0.18409(9)	1.02541(9)	4.58(3)
S2	0.2292(2)	0.42192(9)	0.84091(9)	4.68(3)
O	-0.0878(7)	0.0511(3)	0.8847(3)	7.8(1)
O1	0.2489(5)	0.1480(2)	1.0039(2)	4.21(7)
O2	0.1751(5)	0.3524(2)	0.9196(2)	4.44(7)
C	-0.0245(8)	0.1167(4)	0.8922(4)	5.0(1)
C11	0.349(1)	0.2557(5)	1.1146(5)	8.3(2)
C12	0.5758(9)	0.0767(4)	1.0853(5)	7.3(2)
C21	0.035(1)	0.5311(4)	0.8400(5)	7.0(2)
C22	0.4130(9)	0.4674(5)	0.8863(5)	6.9(2)
Molecule B				
Ru	0.34590(6)	0.75912(3)	0.61148(2)	3.846(8)
Cl1	0.5169(2)	0.8783(1)	0.6213(1)	6.29(3)
Cl2	0.1676(2)	0.64249(9)	0.5921(1)	5.45(3)
Cl3	0.5665(2)	0.6390(1)	0.69852(9)	6.08(3)
S1	0.1251(2)	0.83954(9)	0.43164(8)	4.38(3)
S2	0.6007(2)	0.61606(8)	0.47028(8)	3.86(2)
O	0.092(1)	0.8295(4)	0.7700(3)	9.6(2)
O1	0.1511(6)	0.8617(2)	0.5288(2)	4.74(8)
O2	0.5192(5)	0.7241(2)	0.4913(2)	4.22(7)
C	0.1875(9)	0.8004(4)	0.7128(4)	5.0(1)
C11	-0.1303(9)	0.8945(5)	0.4161(4)	6.0(1)
C12	0.232(1)	0.9263(5)	0.3616(4)	6.9(2)
C21	0.4730(7)	0.6079(4)	0.3740(3)	4.4(1)
C22	0.8346(8)	0.6182(4)	0.4167(4)	5.4(1)

^a Anisotropically refined atoms are given in the form of the isotropic equivalent displacement parameter defined as: $(4/3) [a^2\beta(1,1) + b^2\beta(2,2) + c^2\beta(3,3) + ab(\cos \gamma)\beta(1,2) + ac(\cos \beta)\beta(1,3) + bc(\cos \alpha)\beta(2,3)]$.

Table 4. Selected Bond Distances (Å) and Angles (deg) for **3**

Ru–Cl1	2.338(1)	S2–C4	1.737(4)
Ru–Cl2	2.348(1)	O2–C2	1.126(6)
Ru–Cl3	2.3299(7)		
Ru–O1	2.130(3)	Ru–O1B	2.23(3)
Ru–C2	1.815(4)	C1–S1B	1.804(8)
Si–O1	1.514(3)	C3–S2B	1.701(7)
Si–C1	1.773(4)	C4–S2B	1.940(7)
S2–O3	1.534(4)	S1B–O1B	1.40(3)
S2–C3	1.775(5)	S2B–O3B	1.62(2)
Cl1–Ru–Cl2	177.81(5)	C3–S2–C4	100.0(2)
Cl1–Ru–Cl3	89.28(3)	Ru–O1–Si	127.1(2)
Cl1–Ru–O1	94.84(9)	Ru–C2–O2	179.0(5)
Cl1–Ru–C2	91.3(2)		
Cl2–Ru–Cl3	90.67(3)	Cl1–Ru–O1B	71.9(8)
Cl2–Ru–O1	83.0(1)	Cl2–Ru–O1B	105.9(8)
Cl2–Ru–C2	90.9(2)	Cl3–Ru–O1B	88.45(3)
Cl3–Ru–Cl3	176.85(4)	C2–Ru–O1B	163.2(8)
Cl3–Ru–O1	88.67(3)	C1–S1B–C1	94.0(5)
Cl3–Ru–C2	91.42(3)	C1–S1B–O1B	102.3(9)
O1–Ru–C2	173.8(2)	C3–S2B–C4	95.0(3)
O1–Si–C1	103.8(2)	C3–S2B–O3B	95.4(8)
C1–Si–C1	96.1(2)	C4–S2B–O3B	98.4(8)
O3–S2–C3	103.6(2)	Ru–O1B–S1B	124.(2)
O3–S2–C4	102.2(2)		

Remarkably, even though this reactivity is similar to that found with nitrogen donor ligands,⁶ coordination of CO induces an S to O linkage isomerization of the remaining DMSO. The main structural features of **3** clearly resulted from its solid state infrared spectrum (Table 6), which showed a strong C–O stretching band and an S–O stretching band for O-bonded DMSO. The metal–ligand stretching region of the spectrum is largely dominated by the very broad O–H–O stretching band

Table 5. Selected Bond Distances (Å) and Angles (deg) for **4** (Two Independent Molecules (A and B) Present in the Unit Cell)

	A	B
Ru–Cl1	2.334(1)	2.306(2)
Ru–Cl2	2.332(1)	2.343(2)
Ru–Cl3	2.304(1)	2.304(1)
Ru–O1	2.049(3)	2.058(3)
Ru–O2	2.126(4)	2.122(3)
Ru–C	1.838(6)	1.865(5)
S1–O1	1.547(4)	1.546(4)
S1–C11	1.737(7)	1.776(6)
S1–C12	1.761(6)	1.772(7)
S2–O2	1.513(3)	1.537(3)
S2–C21	1.769(6)	1.771(5)
S2–C22	1.777(8)	1.772(6)
O–C	1.134(8)	1.095(7)
Cl1–Ru–Cl2	173.83(6)	176.38(5)
Cl1–Ru–Cl3	91.09(5)	92.72(6)
Cl1–Ru–O1	88.03(9)	88.9(1)
Cl1–Ru–O2	90.5(1)	87.6(1)
Cl1–Ru–C	92.2(2)	89.8(2)
Cl2–Ru–Cl3	92.87(5)	90.21(6)
Cl2–Ru–O1	88.01(9)	88.1(1)
Cl2–Ru–O2	84.6(1)	90.2(1)
Cl2–Ru–C	92.6(2)	92.2(2)
Cl3–Ru–O1	179.10(9)	177.2(1)
Cl3–Ru–O2	92.0(1)	91.28(9)
Cl3–Ru–C	89.2(2)	92.6(2)
O1–Ru–O2	88.2(1)	86.5(1)
O1–Ru–C	90.7(2)	89.7(2)
O2–Ru–C	177.0(2)	175.4(2)
O1–S1–C11	104.6(3)	102.3(3)
O1–S1–C12	102.0(3)	103.3(3)
C11–S1–C12	99.6(3)	100.6(3)
O2–S2–C21	104.9(3)	104.3(2)
O2–S2–C22	102.6(3)	102.6(2)
C21–S2–C22	98.2(3)	99.0(3)
Ru–O1–S1	119.4(2)	119.4(2)
Ru–O1–C12	156.0(2)	147.4(2)
S1–O1–C12	42.0(2)	42.1(2)
Ru–O2–S2	122.9(2)	121.7(2)
Ru–O2–C22	153.7(2)	148.3(2)
Ru–C–O	178.0(5)	176.4(5)

of the cation centered around 700 cm^{-1} .¹⁷ Assignments were done more easily on the sodium salt, **3Na**, according to literature reports on Ru–DMSO and Ru–CO complexes.^{6,18} Comparison with the spectrum of the hexadeuterated derivative of **3Na** allowed to distinguish unambiguously the Ru–O stretching band, which is slightly shifted to lower frequencies upon deuteration (isotope ratio 1.05), from $\delta(\text{RuCO})$ and $\nu(\text{Ru–CO})$. We observed that the solid state CO stretching frequency is dependent on the nature of the cation ($2024\text{--}2047\text{ cm}^{-1}$), but falls in the range found in the literature for monomeric Ru(III)–CO compounds ($1985\text{--}2052\text{ cm}^{-1}$). A more reliable value for $\nu(\text{CO})$ (2038 cm^{-1}) was obtained in chloroform solution with the tetrabutylammonium derivative **3NBu₄**.

The unusually high S–O stretching frequency, accompanied by a particularly low-frequency Ru–O stretching, suggested that in **3** DMSO is coordinated weakly to ruthenium. This feature is in agreement with the results of the X-ray crystal structure determination (Figure 2). In fact, the Ru–O bond length of $2.130(3)\text{ Å}$ in **3** is considerably longer than those of $2.077(3)$ and $2.070(2)\text{ Å}$ found in **2**⁵ and in *mer,cis*-RuCl₃(DMSO)(DMSO)(NH₃),⁶ respectively, which represent the only other source of structural data on the Ru(III)–DMSO bond. This is to be attributed to the greater trans influence of CO compared

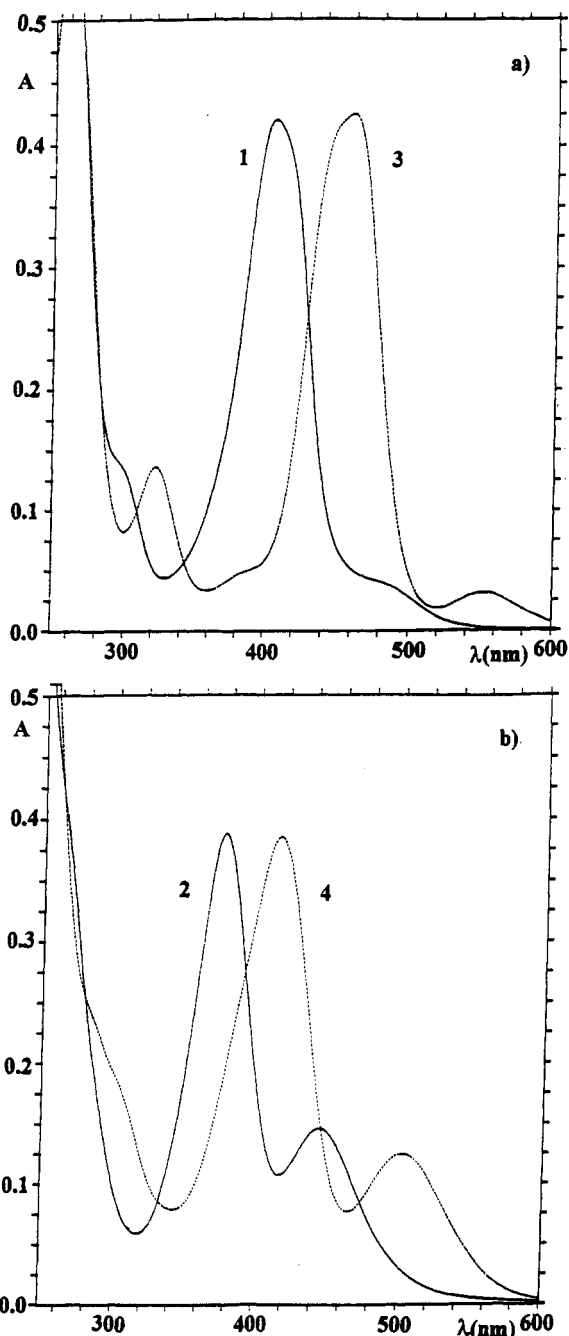


Figure 1. (a) Electronic absorption spectra of **1NBu₄** (full line) and **3NBu₄** (dotted line) at isocromic concentrations in CHCl₃. (b) Electronic absorption spectra of **2** (full line) and **4** (dotted line) at isocromic concentrations in CHCl₃.

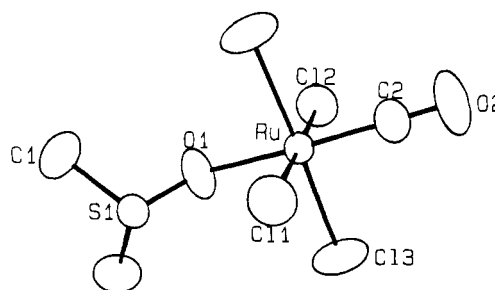


Figure 2. ORTEP drawing of **3** with the atom-labeling scheme.

to Cl. In agreement with the binding model for DMSO,¹⁹ which involves a lengthening of the S–O bond distance upon

(17) James, B. R.; Morris, R. H. *Can. J. Chem.* **1980**, *58*, 399.

(18) Cleare, M. J.; Fritz, H. P.; Griffith, W. P. *Spectrochim. Acta* **1972**, *28A*, 2019.

(19) Davies, J. A. *Adv. Inorg. Chem. Radiochem.* **1981**, *24*, 115.

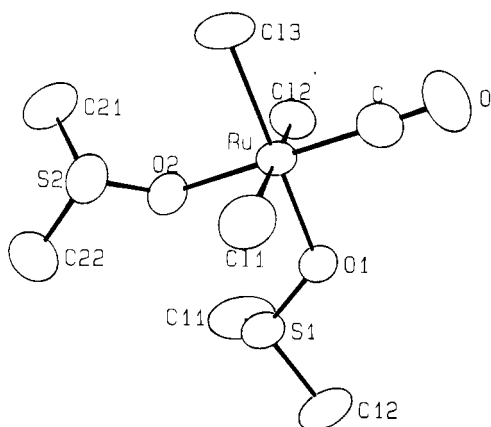


Figure 3. ORTEP drawing of **4** with the atom-labeling scheme.

Table 6. Selected IR Absorption Bands of Ruthenium(III) Carbonyl Complexes **3–6** (cm^{-1})

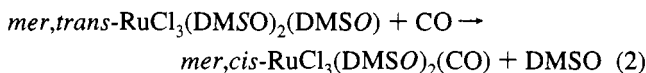
complex	ν_{CO}	$\nu_{\text{SO DMSO}}$	δ_{RuCO}	$\nu_{\text{Ru-C}}$	$\nu_{\text{Ru-O}}$	$\nu_{\text{Ru-Cl}}$
3	2030 (vs)	957 (s)			461 (m)	320 (s)
3Na	2047 (vs)	928 (s)	549 (m)	503 (w)	476 (m)	326 (s)
3NBu₄	2024 (vs)	954 (s)			465 (m)	324 (s)
4	2044 (vs)	932, 885 (s)	550 (m)	500 (w)	510, 485 (m)	339 (s)
5	2025 (vs)		538 (m)			320 (s)
6	2054 (vs)	883 (s)	534 (m)		513 (m)	331 (s)

increasing the M–O bond strength, the weakening of the M–O σ bond in **3** yields to an S–O distance of 1.514(3) Å, which is significantly shorter than those found in **2** (1.545(4) Å)⁵ and in *mer,cis*-RuCl₃(DMSO)(DMSO)(NH₃) (1.547(2) Å).⁶

The structural parameters of CO in **3** (Ru–C 1.815(4) Å, C–O 1.126(6) Å) can be appropriately compared with those of [pyH][*trans*-RuCl₄(CO)(py)], whose crystal structure has been recently determined (Ru–C 1.869(7), C–O 1.122(9)).²⁰ Rather unexpectedly, while the C–O bond distances in the two complexes are very similar, the Ru–C bond length in the pyridine derivative is longer than in **3**.

The CDCl₃ ¹H NMR spectrum of **3NBu₄** shows, beside the peaks of the cation, a broad resonance centered at –0.2 ppm, that could be unambiguously assigned to DMSO by comparison with the DMSO-*d*₆ derivative. Partial dissociation of this ligand is deduced by the presence of the resonance of free DMSO. DMSO dissociation is immediate and complete in D₂O solution.

The reactivity of the neutral Ru(III) derivative **2** with carbon monoxide at room temperature and atmospheric pressure is similar to that of **1**, involving the replacement of one of the two trans S-bonded DMSO ligands accompanied by the linkage isomerization of the remaining DMSO to give **4** (eq 2). Also



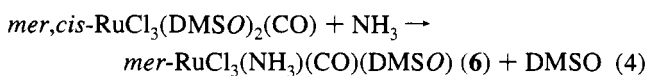
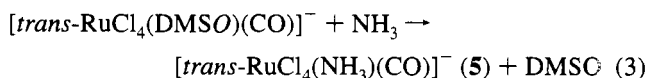
in this case replacement of DMSO with a stronger π -acceptor ligand involves a red-shift in the visible spectrum of the complex compared to its precursor (Figure 1b). The presence of coordinated CO and of exclusively O-bonded DMSO in **4** was clearly indicated by its IR spectrum (Table 6) and confirmed by its crystal structure (Figure 3). IR assignments have been confirmed by comparison with the corresponding DMSO-*d*₆ derivative.

The CO stretching band in **4** falls at slightly higher frequency compared to that of **3**, and this might be mainly attributed to the net negative charge of the latter complex. We observed

that the shape of the S–O stretching region in the solid state IR spectrum of **4** depends on the preparation. In fact, the raw material usually showed only a very broad band for DMSO centered at 910 cm^{-1} , clearly deriving from the overlap of several bands; they could be sometimes partially resolved in two still broad bands centered at 932 and 885 cm^{-1} . These two bands became rather narrow and completely resolved when the product crystallized slowly from the mother liquor of the synthesis. On the other hand, the different batches gave superimposable spectra in solution (UV–vis, NMR, IR), suggesting that, in analogy to what observed with *cis*-RuCl₂(DMSO)₄,¹ the solid state IR features observed in the S–O stretching region might be attributed to the presence of atropisomers differing from each other in the orientation of the DMSO ligands. As reported above for **3**, we attributed the S–O stretching band of higher frequency, together with the Ru–O stretching band of lower frequency, to the less tightly bonded DMSO, that is the one trans to carbon monoxide. This attribution is in agreement with the structural data, which show that the Ru–O bond distances trans to CO, in both the crystallographically independent molecules, are similar to those found in **3** and considerably longer than those trans to Cl (average 2.124(3) vs 2.054(6) Å). Correspondingly, the S–O distances in the less tightly bonded DMSO are slightly shorter than in the other (average 1.525(17) vs 1.547(1) Å). Again, this difference between the two DMSO ligands can be attributed to the difference of trans influence between CO and Cl. Interestingly, the DMSO trans to Cl in **4** is more tightly bonded than in the precursor **2** (*d*(Ru–O) average 2.054(6) vs 2.077(3) Å). This might be attributed to the greater steric hindrance exerted by the two DMSO ligands in **2** compared to CO and DMSO in **4**.²¹

The ¹H CDCl₃ spectrum of **4** shows two equally intense broad peaks centered at –0.33 ppm and 7.20 ppm (–0.30 ppm and 6.95 ppm in CD₂Cl₂) for the two DMSO ligands. Dissociation of DMSO was not observed in aprotic solvents. In accordance with the spectrum of **3**, we attributed the high field resonance to the DMSO trans to CO. In further agreement with this assignment and with the expected lower bond strength of this DMSO compared to that trans to Cl, in D₂O solution only the resonance at low field (DMSO trans to Cl, 8.70 ppm) is present, while the high field resonance disappears and is replaced by the peak of free DMSO at 2.71 ppm.

Reactivity of **3 and **4** with Nitrogen Ligands.** The reactivity of the precursors **1** and **2** with uncharged nitrogen donor ligands (N) has been already reported by us.⁶ As a comparison, we investigated also the reactivity of **3** and **4** with the same ligands. In particular we focused on ammonia, but a similar reactivity was observed with other ligands such as pyridine (supporting information). As expected from the above considerations concerning the strength of the Ru–DMSO bond, both **3** and **4** react quite easily with gaseous ammonia, stereoselectively replacing the DMSO trans to CO to give **5** and **6**, respectively (eqs 3 and 4). Combined spectroscopic evidence (IR, NMR,



UV–vis) suggested that the geometry of the complexes was

(20) (a) Keppler, B. K.; Lipponer, K. G.; Stenzel, B.; Kratz, F. In *Metal Complexes in Cancer Therapy*; Keppler, B. K., Ed.; VCH: Weinheim, Germany, 1993; p 189; (b) Keppler, B. K. Personal communication.

(21) Calligaris, M.; Faleschini, P.; Todone, F.; Alessio, E.; Geremia, S. J. *Chem. Soc., Dalton Trans.* **1995**, 1653.

maintained in the reaction. For example, the shape of the visible spectra of the products remained almost unaltered compared to the precursors, except for a slight shift to higher frequencies. In the case of the neutral compound **4**, however, either the DMSO trans to CO or that trans to Cl might, in principle, undergo substitution. Even in the absence of a crystal structure, the geometry of **6** was unambiguously determined from combined IR and ^1H NMR evidence. The complex, in fact, has only the low frequency S–O stretching (883 cm^{-1}) and the low field resonance (8.1 ppm, confirmed by comparison with the DMSO- d_6 derivative) attributed in **4** to the DMSO trans to Cl.

Substitution of DMSO with the nitrogen ligand did not involve significant changes in the CO stretching frequencies (Table 6).

The neutral derivatives *mer*-RuCl₃(N)(CO)(DMSO) are reported here for the first time. In the case of the anionic complexes, when N = pyridine our method is an alternative route to the synthesis of [*trans*-RuCl₄(CO)(py)][−], which had been previously synthesized as pyridinium salt.¹³ Our procedure, however, is quite general for anionic compounds of formula X[*trans*-RuCl₄(CO)(N)] and allows one to select the nature of the cation and therefore the solubility of the product.

Discussion

In agreement with what we had already reported,⁶ the reactivity of [(DMSO)₂H][*trans*-RuCl₄(DMSO)] (**1**) and *mer*-, *trans*-RuCl₃(DMSO)₂(DMSO) (**2**) with neutral ligands is determined by the rather strong trans-effect of S-bonded DMSO and consists in the stereoselective replacement of the DMSO ligand trans to DMSO. When the entering ligand (L) is a pure σ -donor, such as ammonia, substitution occurs without affecting the binding mode of the remaining sulfoxides.⁶ However, when L is a strong π -acceptor such as CO, the substitution involves also the S to O isomerization of the DMSO trans to it.

Examples of DMSO linkage isomerization induced by a change in the oxidation state of the metal center²² (e.g. [Ru(NH₃)₅(DMSO)]²⁺ vs [Ru(NH₃)₅(DMSO)]³⁺) or by a change in the electron-withdrawing properties of the ancillary ligand²³ (e.g. Rh₂(O₂CCH₃)₄(DMSO)₂ vs Rh₂(O₂CCF₃)₄(DMSO)₂) or by a change in the geometry of the complex^{1,7} (e.g. *cis*,*fac*-RuCl₂(DMSO)₃(DMSO) vs *trans*-RuCl₂(DMSO)₄ and *mer*,*cis*-RhCl₃(DMSO)₂(DMSO) vs *mer*,*trans*-RhCl₃(DMSO)₂(DMSO)) have been previously reported. However, the effect of the coordination of a strong π acceptor on the DMSO bonding mode is unprecedented and contributes to the understanding of the nature of the metal–DMSO bond. The preference of coordinated DMSO either for S- or O-bonding is usually attributed to a balance of electronic and steric factors.¹⁹ As a general rule, the less polarizable (usually smaller and/or more highly charged) metal ions prefer O-bonding, while the more polarizable (usually larger and/or less charged) metal ions prefer S-bonding. O-bonded DMSO is also less sterically demanding than DMSO.²¹ When S-bonded, DMSO is generally considered as a relatively weak π -acceptor ligand. In both Ru(II) and Ru(III) derivatives S-bonding seems to be favored for electronic reasons, in particular for neutral or anionic derivatives, oxygen bonding being adopted when the steric crowding around the complex is relevant (such as in **2** or in *cis*,*fac*-RuCl₂(DMSO)₃(DMSO)) or when a positive charge is present^{24,25} (e.g. *fac*-[RuCl(DMSO)₃(DMSO)₂]⁺ and *fac*-[Ru(DMSO)₃(DMSO)₃]²⁺). The sulfur to oxygen isomerization that occurs in **1** and **2** upon replacement

of one of the two *trans* S-bonded DMSO ligands with carbon monoxide can be attributed exclusively to electronic factors since the steric crowding of the complex, which might favor O-bonding, is even reduced compared to the precursors. This brings further evidence to our hypothesis that DMSO acts as a π -acceptor, not only on Ru(II), but also on Ru(III).^{5,6} In the presence of a stronger π -acceptor such as CO, selective S to O isomerization of the DMSO trans to it occurs in order to remove the competition for π -electrons.

The DMSO trans to CO is weakly bonded to ruthenium and we showed that it can be readily replaced by a stronger σ -donor, such as a nitrogen ligand (N). In principle, the two-step sequence that leads to X[*trans*-RuCl₄(N)(CO)] and *mer*-RuCl₃(N)(CO)(DMSO) from the precursors **1** and **2**, that is coordination of CO followed by coordination of the ligand, might be reversed by reacting the precursors with the nitrogen ligand first.⁶ However, substitution by CO of the DMSO trans to a nitrogen ligand in X[*trans*-RuCl₄(N)(DMSO)] and *mer*-, *cis*-RuCl₃(DMSO)(DMSO)(N) is remarkably more difficult compared to when the *trans* ligand is another DMSO. We have been unable to isolate compounds like **5** and **6** by this alternative route, even adopting more drastic reaction conditions such as reacting the complexes with CO in refluxing dimethylformamide.

Finally, the red-shift of the electronic absorption bands induced by coordination of CO deserves a more detailed comment. The absorption bands in the visible region of [*trans*-RuCl₄(L)₂][−] and RuCl₃(L)₃ complexes (L = neutral ligand) have been attributed to charge transfer from the chlorides to the metal atom.²⁶ In particular, the main band is due to an allowed e_u (Cl π) to b_{2g} (Ru d_{π}) transition, while the two minor bands of slightly higher and lower energy are attributed to parity-forbidden transitions. π -Acceptor ligands in octahedral complexes are known to stabilize the t_{2g} levels, thus reducing the energy gap between the two levels and determining the bathochromic shift of the visible bands.

Conclusions

[(DMSO)₂H][*trans*-RuCl₄(DMSO)(CO)] (**3**) and *mer*,*cis*-RuCl₃(DMSO)₂(CO) (**4**) represent the first example of Ru(III)–DMSO–CO derivatives and contribute to the rather limited number of Ru(III)–CO complexes reported to date. The prompt coordination of CO on the Ru(III) precursors **1** and **2** is in agreement with our hypothesis that Ru(III) can be a rather good π base. Selective S to O isomerization of the DMSO trans to CO occurs in order to remove the competition for π -electrons. This confirms that the favored binding mode for DMSO is highly sensitive to moderate changes in electronic structure resulting from alteration of the ligand set. As clearly shown by spectroscopic and structural data, the DMSO trans to CO is weakly bonded to ruthenium and can be readily and stereoselectively replaced by a stronger σ -donor, such as a nitrogen ligand.

Acknowledgment. This work was supported by the Italian Ministry for University and Scientific and Technological Research (40% grant). A generous loan of hydrated RuCl₃ from Johnson Matthey PLC is gratefully acknowledged. The authors are thankful to Dr. B. Keppler for providing unpublished crystal data of [pyH][*trans*-RuCl₄(CO)(py)].

Supporting Information Available: Text giving synthetic procedures and spectroscopic characterization of Na[*trans*-RuCl₄(py)(CO)], [NBu₄][*trans*-RuCl₄(py)(CO)], and *mer*,*trans*-RuCl₃(py)(CO)(DMSO) (1 pp) and tables of anisotropic thermal parameters and H-atom parameters (5 pages). Ordering information is given on any current masthead page.

IC941462E

(22) Yeh, A.; Scott, N.; Taube, H. *Inorg. Chem.* **1982**, *21*, 2542.
 (23) Cotton, F. A.; Felthouse, T. R. *Inorg. Chem.* **1980**, *19*, 2347.
 (24) Barnes, J. R.; Goodfellow, R. J. *J. Chem. Res., Miniprint* **1979**, 4301.
 (25) Davies, A. R.; Einstein, F. W. B.; Farrell, N. P.; James, B. R.; McMillan, R. S. *Inorg. Chem.* **1978**, *17*, 1965.

(26) Duff, C. M.; Heath, G. A. *J. Chem. Soc., Dalton Trans.* **1991**, 2401.